Estonian Journal of Earth Sciences, 2016, **65**, 3, 125–137 doi: 10.3176/earth.2016.11

# Magnetic susceptibility of Middle Ordovician sedimentary rocks, Pakri Peninsula, NW Estonia

Jüri Plado[a], Leho Ainsaar[a], Marija Dmitrijeva[a], Kairi Põldsaar[a], Siim Ots[a], Lauri J. Pesonen[b] and Ulla Preeden[a,c]

[a] Institute of Ecology and Earth Sciences, University of Tartu, Ravila 14A, Tartu 50411, Estonia; juri.plado@ut.ee
[b] Division of Geophysics, University of Helsinki, PO Box 64, FI00014 Helsinki, Finland
[c] Põlva County Government, Kesk 20, Põlva 63308, Estonia

Received 2 February 2016, accepted 23 May 2016

**Abstract.** Magnetic susceptibility (MS), its frequency-dependence and anisotropy of the Middle Ordovician Dapingian and Darriwilian sedimentary sequence from three sites (Uuga, Testepere and Leetse) in the Pakri Peninsula, NW Estonia are analysed in combination with the mineralogical composition. The study is based on 463 cores drilled at intervals of a few centimetres to a maximum of about 1 m. All the samples show low and positive MS, which suggests the presence of small quantities of para- and/or ferromagnetic minerals. The stratigraphic units of the three studied sites have a similar along-section appearance, which provides a base for a composite curve. The relatively higher susceptibilities are carried by secondary Fe–Ti oxides (Toila Formation), goethite ooids (Kandle Formation) and ferrous dolomite (Pae Member), whereas paramagnetic minerals are mostly responsible for the rest of the sequence. Considering the dependence of MS on regressive–transgressive cycles (high/low MS within deposits of regressive/transgressive parts of the cycles, respectively), the MS data do not agree with sedimentologically derived sea-level compilations. The measured changes in MS in the Pakri Peninsula outcrops correlate at certain characteristic levels with those deposited in the deeper part of the palaeobasin (Viki core), indicating that the post-depositional iron mobilization within the sediments took place at least at a regional level. Because of post-depositional reorganization of ferromagnetic carrier minerals, the MS values may, however, not be used as a detrital proxy.

**Key words:** magnetic susceptibility, carbonate rocks, Ordovician, Estonia.

## INTRODUCTION

The terrain of the Baltica palaeocontinent occupies the landmass in northern and eastern Europe in between the Ural Mountains and the Trans-European Suture Zone. The East European Craton (EEC) forms the core of Baltica and has a thick Archaean to mid-Proterozoic continental crust (Bogdanova et al. 2006). The Ediacaran to Palaeozoic sediments are widely distributed and form a number of distinct basin depocentres within the supracrustal successions of the EEC (see Nikishin et al. 1996 for details).

The Baltoscandian Palaeobasin (Fig. 1A) developed in the western part of the EEC and at times extended to more or less the areas of present-day NW Russia, the Baltic States, Scandinavia, Poland and Belarus (Männil 1966; Jaanusson 1973). It has been a stable intracratonic sedimentary basin through most of its evolution. In the northern and central parts of the basin (Estonia, northern Latvia and NW Russia), the Ediacaran and lower Palaeozoic sediments cover the Precambrian crystalline basement (Nikishin et al. 1996). In Estonia, the Ediacaran to Devonian sediments lie on the southern slope of the Baltic Shield and are slightly (<1°) tilted southwards. The deposits are well preserved and unaffected by deep burial diagenesis and significant tectonic deformations. The sediments are, however, not pristine and have undergone diagenetic processes varying in intensity both vertically and laterally (Vingisaar & Taalmann 1974; Kirsimäe et al. 1999; Raidla et al. 2006). The area under study was a shallow marine carbonate facies known as the North Estonian Confacies or the Estonian Shelf (Nestor & Einasto 1997; Fig. 1A) during the Middle Ordovician. The Baltoscandian Palaeobasin, together with the Baltica Plate, was shifting northwards from about 50° to 30° southerly latitudes during the Middle Ordovician (Torsvik et al. 2012; Plado et al. 2016) and probably experienced a temperate climate (Lindström 1984).

Magnetic properties often provide proxy information of the concentration and composition of the depositing material and their use has become widespread in the study of Phanerozoic sediments (e.g. da Silva & Boulvain 2006). Magnetic susceptibility (MS) has often been used

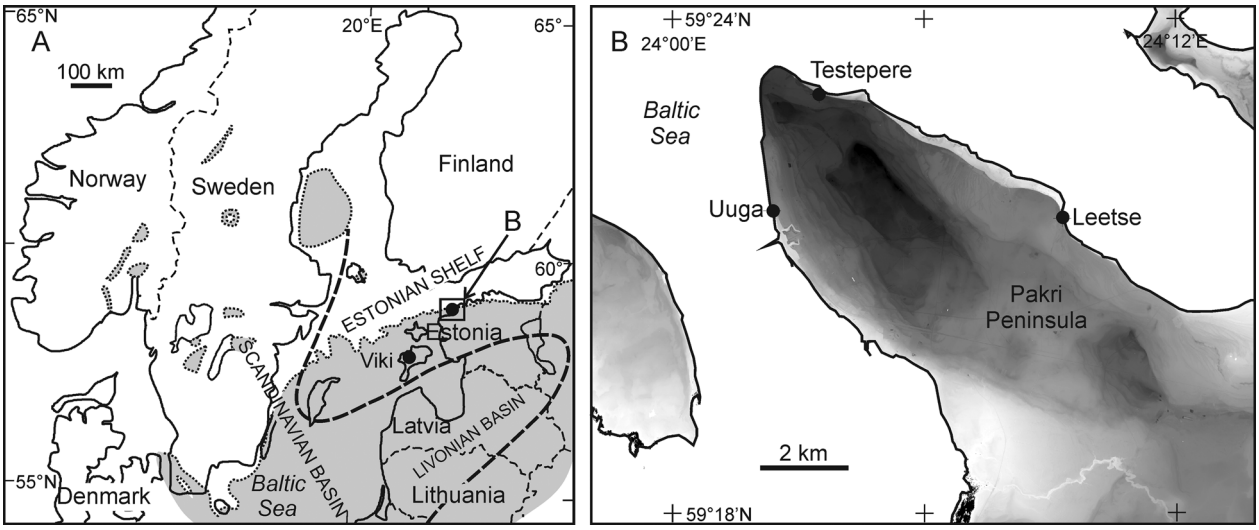


**Fig. 1.** (**A**) Location of the study area in the Scandinavian–Baltic area. The dashed line is the outline of the Swedish–Latvian Confacies Belt including the Scandinavian and Livonian basins (Baltoscandian Palaeobasin; after Männil 1966 and Jaanusson 1973). Light grey highlights the distribution of Ordovician deposits. (**B**) Location of the Uuga, Testepere and Leetse outcrops on the Pakri Peninsula. Grey tones reflect topography (from 0 [white] to ~30 m [black]).

for correlative purposes because magnetic correlations are intercontinental and provide better precision than biozones (Crick et al. 1997, 2000; Ellwood et al. 2000; Whalen & Day 2008, 2010). It has been suggested that variations in MS are related to changes in lithogenic (aqueous, detrital and aeolian) inputs during transgressive–regressive cycles, which in turn results in changes in the amount of iron, clay and ferromagnesian constituents (e.g. Ellwood et al. 2006). Sequence stratigraphic analyses have shown that during lowstand and early transgressive episodes the erosion of continents increases an influx of detrital material into basins, whereas the MS high during early transgression is likely the result of transgressive reworking of high MS detrital components eroded during lowstand (Racki et al. 2002; Whalen & Day 2010). On the contrary, low MS is generally observed within deposits of late transgressive and highstand parts of the cycles. Major eustatic sea-level fluctuations are related to palaeoceanographic changes, which are recorded in the stable isotope composition of the corresponding sedimentary rocks and are represented by biotic changes (see Ainsaar et al. 2010).

Post-sedimentary processes may change the depositional magnetic signal. For example, during diagenesis, the magnetic properties of marine sediments may be modified by (i) the conversion of ferromagnetic minerals into paramagnetic phases, (ii) formation of new iron sulphide minerals by metabolic activity of sulphate-reducing microbial organisms (Maloof et al. 2007), (iii) sulphide oxidation (Suk & Halgedahl 1996) and (iv) illitization of smectite which liberates iron and creates suitable conditions for the formation of iron oxides and hydroxides (e.g. Hirt et al. 1993). None of the above processes significantly changes the total amount of iron that is present in the sediments. Studies by Maloof et al. (2007) have proven that early-cemented peritidal carbonates are likely to preserve syndepositional magnetofossil stratigraphies during early diagenesis. Nevertheless, elevated temperature, stress and chemical activity are individually, or acting in combination, capable of causing changes in magnetic minerals and therefore in MS. If diagenetic processes are similar in different parts of a depositional basin, MS provides a basis for basinwide correlations (e.g. correlation across the western Canada sedimentary basin; Whalen & Day 2008, 2010).

Here we report MS logs of the Dapingian and Darriwilian (Middle Ordovician) sedimentary carbonates from three sites of the Pakri Peninsula, NW Estonia, and compare these with earlier studied MS data from the Viki drill core, western Estonia (Plado & Kalberg 2010; Fig. 1). The changes in MS observed within the studied stratigraphic succession are discussed in the context of sea-level changes (Dronov et al. 2011). The ultimate goal of the present and possible future studies is to provide an alternative tool, i.e. MS mapping, for the evaluation of changes in the sedimentary environments in general and for estimating the effects of post-sedimentary processes on the magnetic properties of rocks within the Baltic Basin. The study includes measure-

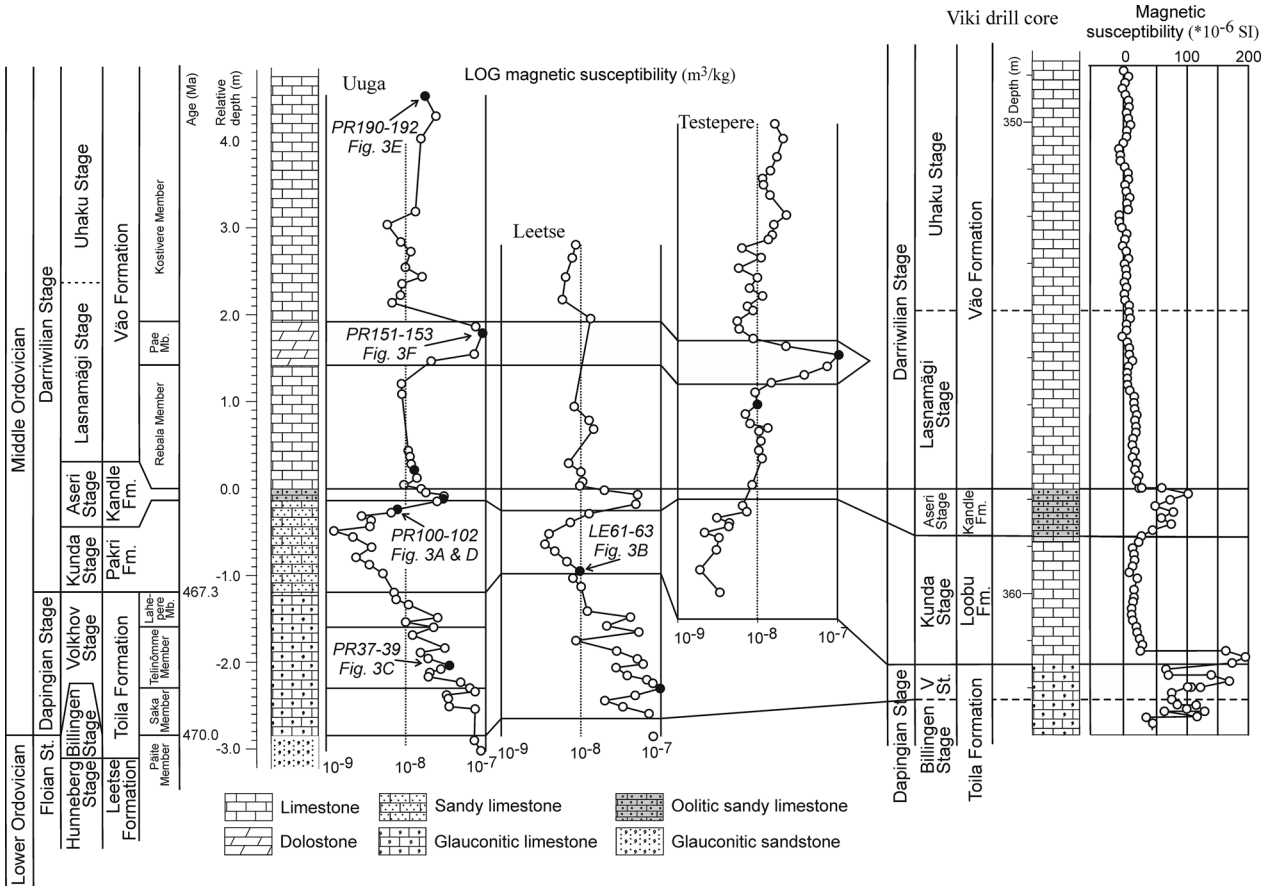


**Fig. 2.** Stratigraphic framework of the Uuga section of the Pakri Peninsula, NW Estonia (after Orviku 1940 and Tammekänd et al. 2010) and along-section variations in the measured low field (1 kHz) magnetic susceptibility in the Uuga, Leetse and Testepere sections (for the location of sections see Fig. 1). Black data points characterize the susceptibility of samples allocated for mineralogical study (a selection of SEM backscatter electron images is given in Fig. 3). On the right side, the stratigraphy of the Viki drill core (for the location see Fig. 1A; Põldvere & Nestor 2010) and its magnetic susceptibility (after Plado & Kalberg 2010) are given.

ments of frequency-dependent susceptibility (at 1 and 16 kHz), the anisotropy of MS (AMS) and mineralogy (SEM-EDS).

The studied Volkhov to Uhaku (Fig. 2) section in NW Estonia formed during a long-term, widespread marine transgression (Haq & Schutter 2008). The corresponding sedimentary succession, however, includes hiatuses that relate to local stratigraphical disconformities and mark the boundaries of depositional sequences (Dronov & Holmer 1999).

## STRATIGRAPHY AND LITHOLOGICAL DESCRIPTION

The three studied sites of the Pakri Peninsula (Uuga and Leetse coastal cliffs and Testepere abandoned quarry; Fig. 1B) expose the Lower to Middle Ordovician siliciclastic-carbonate succession (Fig. 2). From the oldest to youngest the strata include (Põldsaar & Ainsaar 2014): (i) glauconitic sandstones and limestones of the Toila Formation (Billingen and Volkhov regional stages), (ii) interbedded sandy limestones of the Pakri Formation (Kunda Regional Stage), (iii) a distinct iron oolitic limestone bed of the Kandle Formation (Aseri Regional Stage) and (iv) relatively thick-bedded and hard bioclastic limestones of the Väo Formation (Lasnamägi and Uhaku regional stages). The studied succession is underlain by weakly or moderately consolidated glauconite sandstones of the Leetse Formation (Hunneberg Regional Stage) and overlain by Quaternary sediments (Fig. 2). (For brevity, hereafter we use 'stage(s)' instead of 'regional stage(s)'.) Overlying the >0.3 m thick bed of glauconitic sandstone of the Billingen Stage, the sequence of the Volkhov Stage is up to 1.7 m thick. It is divided into the Saka, Telinõmme and Lahepere members, and consists

of glauconiferous limestone with terrigenous content increasing upwards. The lowermost, Saka Member, is almost pure greenish-grey medium-bedded dolomitized glauconitic limestone, while the Telinõmme Member following upwards is characteristically limestone and marl intercalation and the topmost Lahepere Member has increased sand content. The 0.5–1.5 m thick Pakri Formation of the Kunda Stage overlies the glauconite-rich limestone of the Volkhov Stage. The Pakri bed is represented by sandy limestone and moderately consolidated limy sandstone. The slight kerogen admixture gives these, often heavily bioturbated sandy sediments, a brownish-green pyrite-mottled appearance. Additionally, this part of the succession contains extensive soft-sediment deformation structures throughout the study area, which have been associated with an impact-induced catastrophic earthquake event (Suuroja et al. 2003; Alwmark et al. 2010; Põldsaar & Ainsaar 2014). The overlying thin (~6 cm) layer of undisturbed bioclastic limestone of the Kandle Formation belongs to the Aseri Stage. This layer is lithologically distinct due to the occurrence of numerous unevenly distributed brown iron ooids (Orviku 1940). Light grey skeletal limestone (wackestone-packstone) of the Väo Formation, up to 4.5 m in total thickness, represents the topmost part of the studied succession. The skeletal grains vary in size and are partly pyritized. This formation includes the whole Lasnamägi Stage and the lower part of the Uhaku Stage. The Väo Formation can be subdivided, from the oldest to youngest, into the Rebala, Pae and Kostivere members. The lower and upper members are characteristically pure limestones, whereas the middle Pae Formation is thoroughly dolomitic (Tammekänd et al. 2010). Thus, despite the numerous sedimentary hiatuses in the section, the succession of the Pakri Peninsula represents stratigraphically almost the entire Middle Ordovician Series.

## METHODS

The study is based on 463 cores drilled at variable intervals, ranging from a few centimetres to a maximum of about 1 m at three different locations (Figs 1, 2) on the Pakri Peninsula, NW Estonia. Cores with ~25 mm diameter were collected in 2011 using a gasoline-powered drilling machine. The cores were oriented using both magnetic and sun compasses. Three to six horizontally parallel or semi-parallel cores were drilled into individual sedimentary rock layers, and one to four standard 22 mm long specimens were made from each core. Such a technique resulted in 921 specimens. Magnetic susceptibility of the specimens was measured using an SM-100 device (Zh-instruments, Czech Republic) at an alternating magnetic field of 160 A $m^{-1}$ at 1 (low field) and 16 (high field) kHz in the Department of Geology, University of Tartu. The specimens were weighed and MS values were normalized with respect to sample mass (hereafter MS in $m^3$ $kg^{-1}$). Each specimen was measured three times and the mean and standard deviation of these measurements were calculated. Magnetic susceptibility data are also represented as

$$\delta MS = \frac{MS - MS_{\text{marine standard}}}{MS_{\text{marine standard}}},$$

where $MS_{\text{marine standard}} = 5.5 \times 10^{-8}$ (the median value of ~11 000 lithified marine sedimentary rocks, including siltstone, limestone, marl and shale samples; Ellwood et al. 2011). Frequency-dependent susceptibility (Dearing 1999) and total derivative (maximum gradient, defined as the root of the sum of the squared first horizontal derivative and squared first vertical derivative) along the sections were calculated. The anisotropy of MS (AMS) was measured on all cylindrical specimens from the Uuga outcrop (Fig. 1) using a Kappabridge KLY-3 (with 15 sample positions) operating at the Division of Geophysics and Astronomy, University of Helsinki, Finland. The directions of the principal axes of MS ($K_{MAX}$, longest axis; $K_{INT}$, intermediate axis; $K_{MIN}$, shortest axis) were plotted on equal-area stereographic plots. The distribution of the principal axes per locality was highlighted using mean tensor and confidence ellipses. Mean directions, the degree of anisotropy (*Pj*) and the mean shape parameter (*T*) were calculated using Jelinek (1981) statistics by software package 'Anisoft 42', by AGICO Inc.

The chemical composition of 10 samples (the relevant stratigraphical positions are indicated as black dots in Fig. 2) was analysed using variable pressure Zeiss EVO MA15 scanning electron microscope (SEM) equipped with Oxford X-MAX energy dispersive detector system (EDS) at the Department of Geology, University of Tartu. Analyses were conducted in the variable-pressure regime on uncoated polished rock slabs. Spectra were afterwards processed using the Aztec software.

## RESULTS

### Composition of mineralogical phases

The mineral phases were identified using their characteristic chemical composition in order to decipher the magnetic signal carrying minerals within the studied succession. The in-depth mineralogical analysis is out of

the scope of this study and will be conducted elsewhere. All SEM-studied samples are fossil-bearing limestones, sandy limestones or dolostones. The bioclastic detritus is commonly composed of calcite and/or apatite.

The most common Fe-mineral in the studied rocks is represented by fine-grained (typically 1–3 μm, but occasionally <1 μm) iron sulphides, whose composition corresponds to that of pyrite. Iron sulphides are present within the sedimentary matrix (Fig. 3A) as scattered euhedral cubic-octahedral crystallites, framboid aggregates or bundles (concretions) of framboidal aggregates. Scattered pyrite crystals of typically <1 μm gain size are also encountered within bioclastic material (Fig. 3B). Well-developed crystal shapes and especially framboid aggregates suggest an early diagenetic origin of pyrite. The pyrite was detected as the major Fe-mineral in carbonates of the Pakri Formation that also show very low MS values (Fig. 2). This is due to the fact that the pyrite is a paramagnetic mineral and influences the magnetic susceptibility of the whole rock less than ferromagnetic minerals.

Besides pyrite, all of the studied samples also contain iron-titanium oxides with a variable Fe/Ti ratio scattered as micrometre-sized or smaller possibly detrital particles within the calcite or dolomite matrix (Fig. 3C). Pure Fe oxides as single particles are rare and the Fe–Ti oxides or Ti oxides are commonly found but at a far lesser frequency than iron sulphides. In the quartzose sandy limestone of the Pakri Formation, Fe–Ti oxides have often precipitated as encrustations around quartz grains (Fig. 3D). In the Saka Member occasional crystal aggregates of euhedral barite were found occupying the pore space in dolomites (Fig. 3E). Barite occurrence in carbonate rocks can be associated with barite authigenesis in pelagic marine sediments or with late diagenetic/ hydrothermal processes (Griffith & Paytan 2012).

Other potential minerals affecting the MS of the studied strata are ferriferous glauconite, iron ooids and ferroan dolomite. Glauconite grains (up to ca 200 μm in diameter) are abundant in the Saka and Lahepere members of the Volkhov Stage. Glauconite has paramagnetic properties, but it may serve as host for small magnetic (magnetite) grains (see e.g. Lurcock & Wilson 2013). Unlike other studied samples, the Kandle Formation (Aseri Stage) contains abundant ferriferous ooids. These ooids are of iron oxyhydroxide (Sturesson & Bauert 1994) composition. The upper section of the studied stratigraphic interval, especially the Pae Member of the Väo Formation, is heavily dolomitized. There, rhombic ferroan dolomite (Fig. 3F) crystals with the size up to 500 μm have undergone multi-phase growth as seen by the zoning of bright and dark grey areas corresponding, respectively, to Fe-rich and Fe-poor dolomites.

**Magnetic susceptibility**

All the samples show low and positive MS, which suggests the presence of small quantities of para- and/or ferromagnetic minerals. Stratigraphic units of the three studied sites show similar along-section variations in MS (Fig. 2). The similarity gives a base for a composite curve (Fig. 4). From base to top, through the glauconitic limestones of the Toila Formation, there is a decrease in MS until the central part of the Pakri Formation (sandy limestone). As the terrigenous content is highest in the Telinõmme Member (Orviku 1960; Meidla et al. 1998), this trend contrasts the theoretical relationship (high MS ≈ high terrigenous content; see e.g. Śliwiński et al. 2012) and gives a hint of the activity of MS-influencing secondary processes. Indeed, the relatively high MS in the Saka Member is attributable to Fe–Ti oxides that have been precipitated as encrustations around the mineral grains and are of secondary origin according to mineralogical studies (Fig. 3D). In the uppermost half of the Pakri Formation, the MS increases and reaches a peak value (still less than marine standard) in oolitic sandy limestone of the Kandle Formation. Most of the MS peak associated with the Kandle Formation is due to high content of ferriferous (goethite) ooids and Fe–Ti encrustations. A slight upward increase in MS takes place in the limestones of the Väo Formation. This part of the succession shows a sharp positive excursion over the marine MS standard. The excursion corresponds to the dolostones of the Pae Member and is likely caused by a high content of secondary ferroan dolomite.

The curve of the total derivative of MS (Fig. 4) highlights sections where MS varies most abruptly. These are the Saka and Telinõmme members of the Toila Formation, the uppermost part of the Pakri Formation, through the Kandle Formation, and the Pae Member of the Väo Formation. Due to these variations, the MS of these units also has the largest standard deviations compared to the rest of the cross section (Table 1).

Frequency-dependent susceptibility ($MS_{FD}$) was analysed to describe the possible content of superparamagnetic fraction (SP) in the samples (Dearing 1999). Regarding the Päite, Saka and Telinõmme members of the Toila Formation, the values of $MS_{FD}$ are uniform and do not generally exceed 2% (Table 1), hinting at virtually no SP grains. The $MS_{FD}$ value only starts to increase in the upper part of the Toila Formation with glauconitic limestones of the Lahepere Member and reaches the maximum in the Pakri Formation. There, the high $MS_{FD}$ is likely a mathematical artefact caused by magnetically very weak samples. The $MS_{FD}$ values

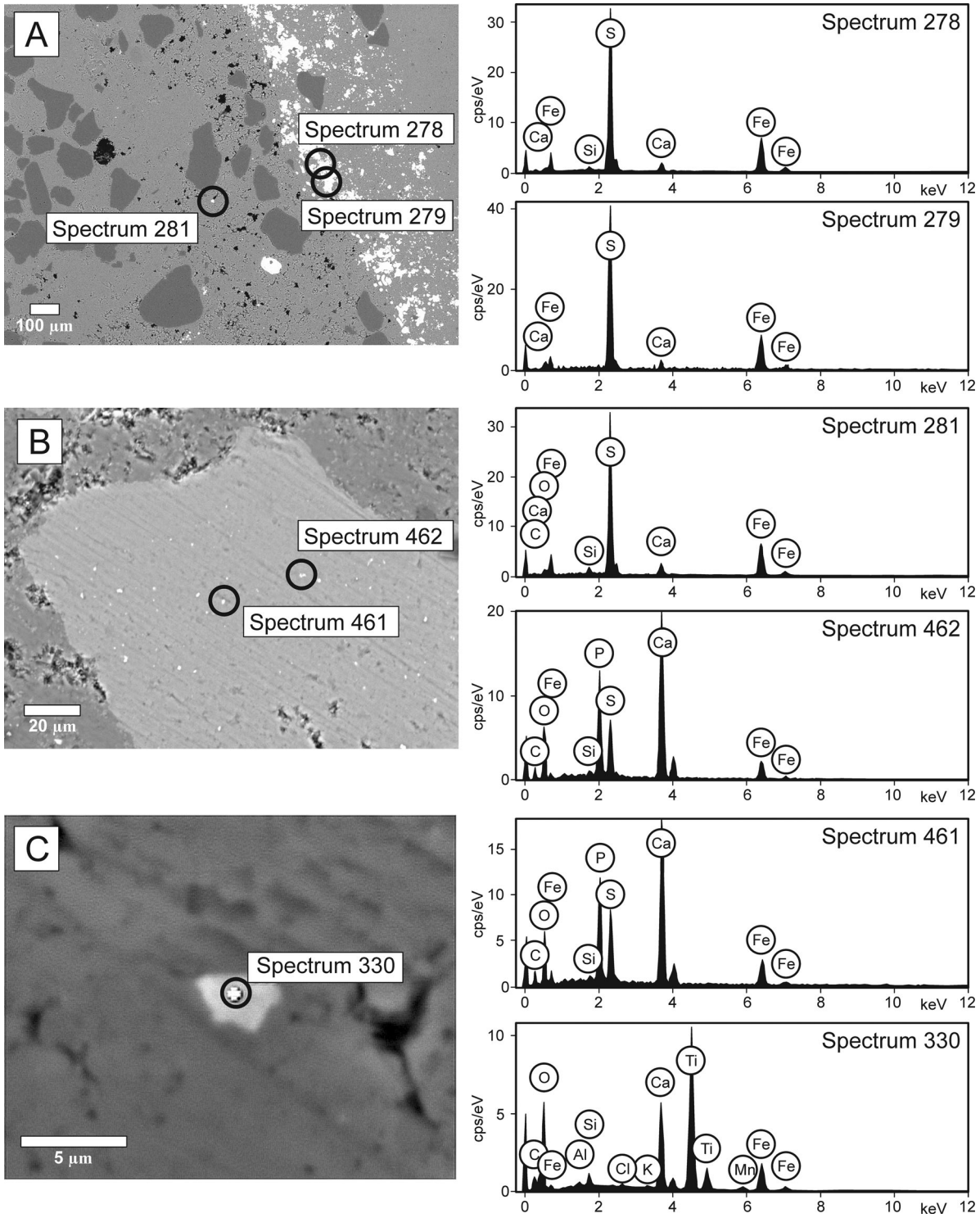


**Fig. 3.** Representative selection of SEM backscatter electron images accompanied with selected spectra of mineral phases of the studied samples. For locations of samples see Fig. 2. **A**, sample PR100-102 (Pakri Formation): iron sulphides are scattered within the calcite matrix; **B**, sample LE61-63 (Pakri Formation): scattered iron sulphide particles of typically <1 μm grain size are encountered within the fossil fragment; **C**, sample PR37-39 (Toila Formation): Fe–Ti oxide grain scattered as a micrometre-sized particle within the calcite or dolomite matrix; **D**, sample PR100-102 (Pakri Formation): Fe–Ti oxide encrustation around a sand grain; **E**, sample PR190-192 (Kostivere Member, Väo Formation): occasional crystal aggregate of euhedral barite occupying the pore space in dolomites; **F**, sample PR151-153 (Pae Member, Väo Formation): dolomite crystals have undergone multiphase growth as seen by bright and dark grey ribbons corresponding to Fe-enriched and Fe-poor dolomite, respectively. Cps, counts per second.

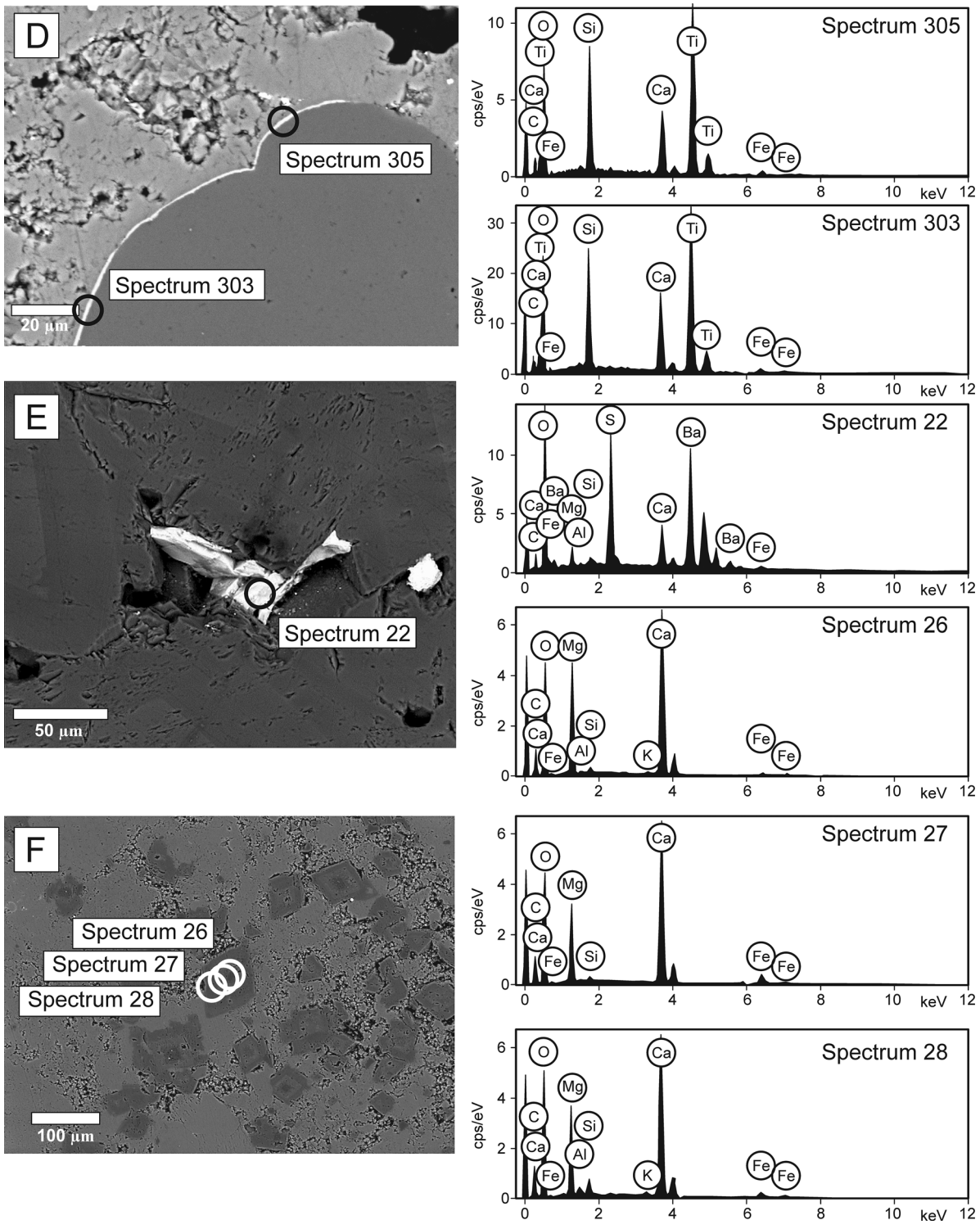


**Fig. 3.** *Continued.*

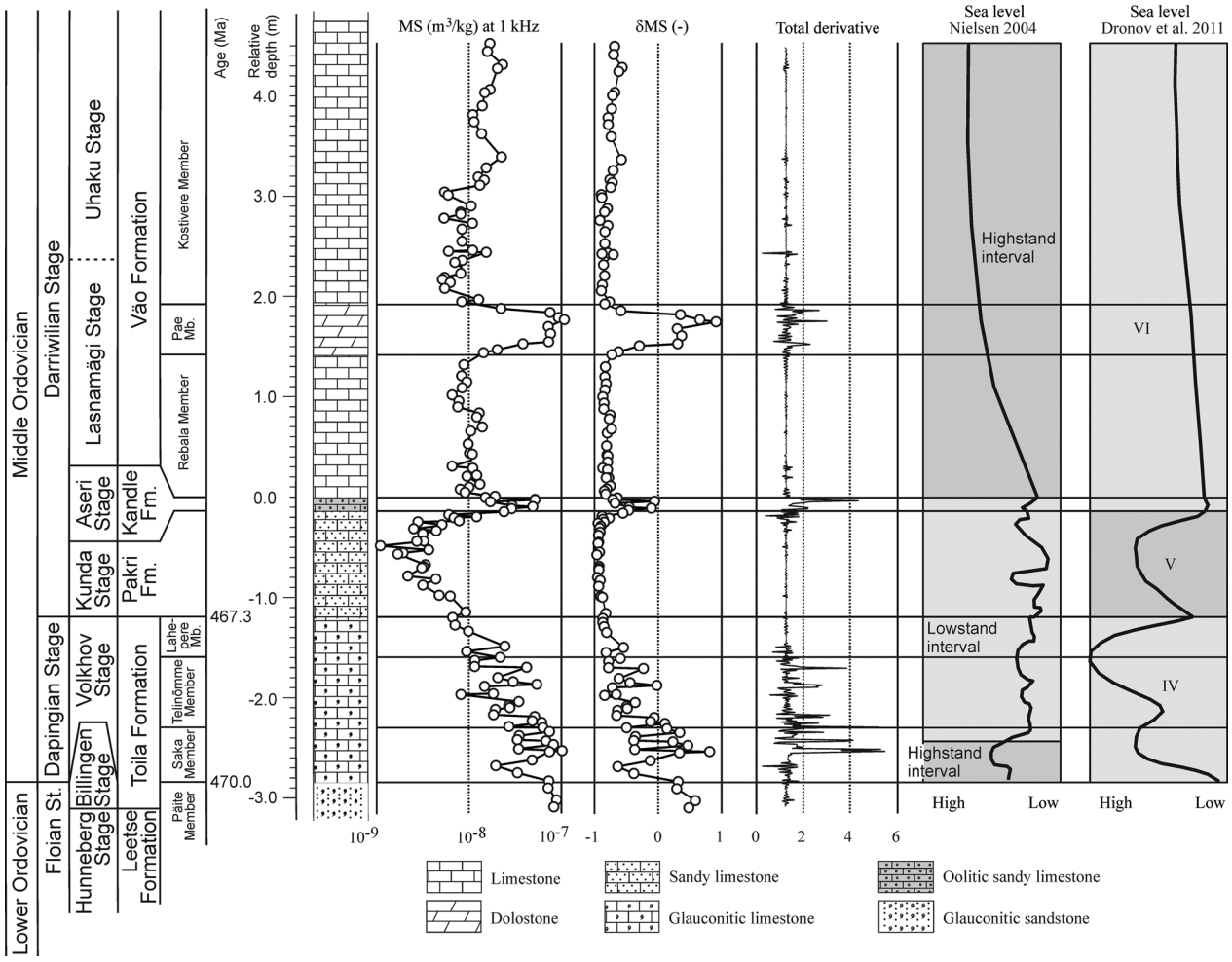


**Fig. 4.** Stratigraphic framework of the Uuga section in the Pakri Peninsula, NW Estonia (after Orviku 1940 and Tammekänd et al. 2010) and along-section variations (i) in the low field (1 kHz) magnetic susceptibility (average data from the Uuga, Leetse and Testepere outcrops), (ii) δMS (see text and Ellwood et al. 2011), (iii) total derivative of (i), (iv) sea-level changes by Nielsen (2004) and (v) sea-level changes by Dronov et al. (2011). See text for explanations of sea-level intervals.

**Table 1.** Average values and standard deviations of magnetic susceptibility (MS) at 1 and 16 kHz, and frequency-dependent susceptibility ($MS_{FD}$) by stratigraphic units; Mb, Member

| | MS ($\times 10^{-9}$ m$^3$ kg$^{-1}$) | | $MS_{FD}$ (%) |
|---|---|---|---|
| | 1 kHz | 16 kHz | |
| Väo Formation | | | |
| Kostivere Mb. | 11.8±4.9 | 11.5±5.0 | 3.2±2.4 |
| Pae Mb. | 58.7±31.8 | 58.1±31.6 | 1.4±0.6 |
| Rebala Mb. | 10.5±2.1 | 10.0±2.1 | 4.3±1.7 |
| Kandle Formation | 30.6±14.8 | 30.0±14.6 | 1.8±0.7 |
| Pakri Formation | 5.5±4.7 | 5.1±4.5 | 7.8±5.5 |
| Toila Formation | | | |
| Lahepere Mb. | 11.4±6.8 | 10.9±6.9 | 4.6±3.4 |
| Telinõmme Mb. | 29.3±15.5 | 28.9±15.4 | 1.7±0.8 |
| Saka Mb. | 56.7±23.7 | 56.2±23.6 | 1.0±0.4 |
| Päite Mb. | 80.0±8.2 | 79.3±7.9 | 0.9±0.6 |

generally stay under 2% in thin oolitic limestones of the Kandle Formation, which is lower than in the overlying Rebala and Kostivere members where some SP grains may occur. Located between the Rebala and Kostivere members, the thoroughly dolomitized Pae Member has low $MS_{FD}$ and no SP grains.

## Anisotropy of magnetic susceptibility

The measured MS is weak for its anisotropy to be measured with high precision. In addition, the magnetic response is complex as the susceptibility carrier is a mixture of para- and ferromagnetic minerals. Generally, for most of the lithological units, the degree of anisotropy (*Pj*; Fig. 5) stays well below 1.02, whereas only the Pakri Formation and Lahepere Member show higher

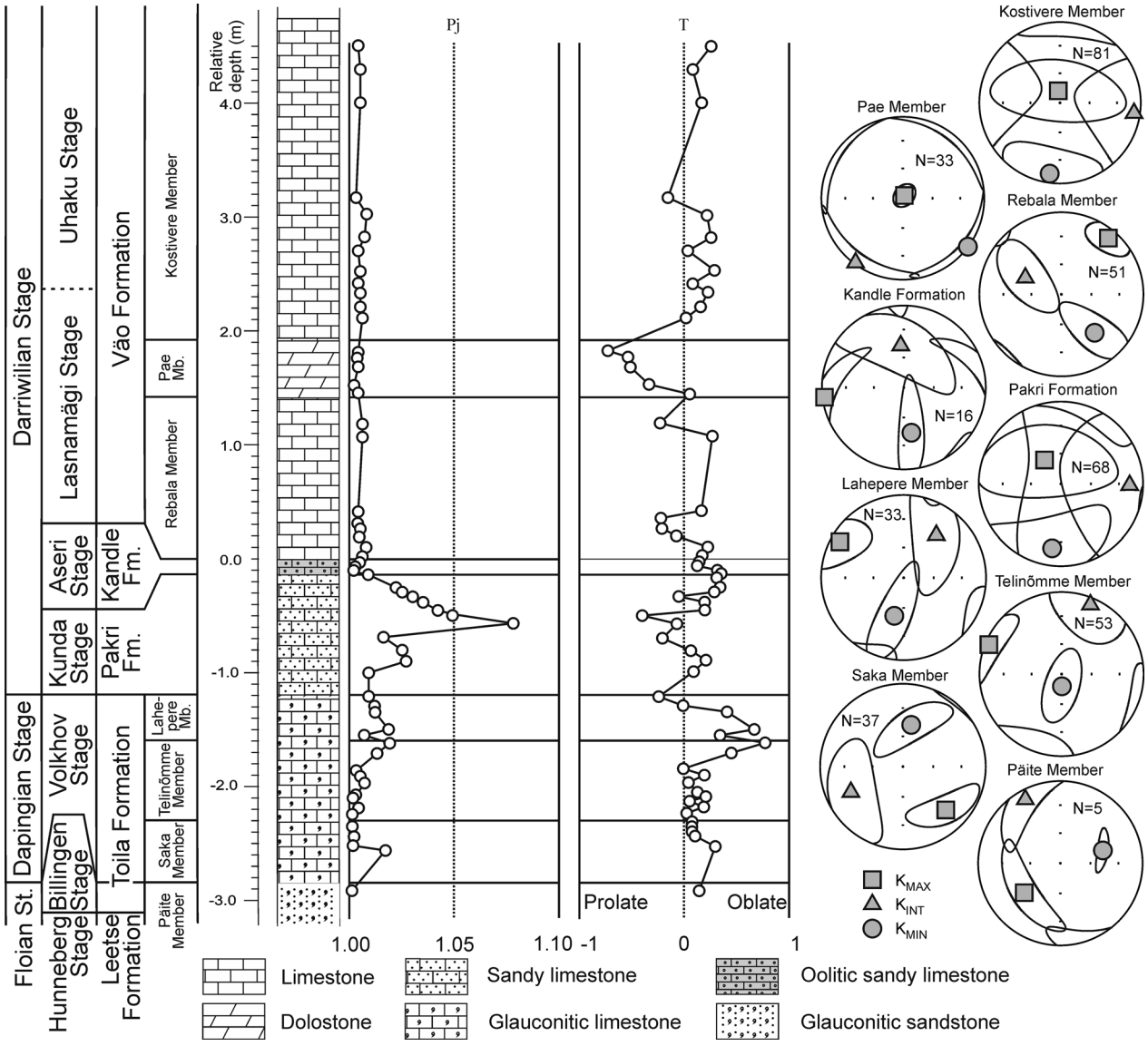


**Fig. 5.** Along-section variations (i) in the degree of anisotropy (*Pj*), (ii) shape parameter (*T*) and (iii) equal area stereographic projections of AMS principal axes ($K_{MAX}$, $K_{INT}$, $K_{MIN}$).

values (up to 1.08 and 1.02, respectively). The shape parameter (*T*) tends to be near zero or slightly positive. That hints at the transitional or weakly oblate shape of the AMS ellipsoid, whereas the horizontal magnetic lineation is (sub)parallel to the bedding plane being maintained by primary sedimentary fabric. A clear exception is the Pae Member where the prolate shape prevails (Fig. 5). The Pae Member, but also the Kostivere Member and the Pakri Formation show an almost vertical longest axis ($K_{max}$) of the MS ellipsoid, hinting directly at post-sedimentary processes that have influenced the MS.

## DISCUSSION

Magnetic susceptibility has proven to be a rapid and reliable tool in solving various problems of stratigraphic correlation including these in ancient sedimentary successions (e.g. da Silva & Boulvain 2006; Ellwood et al. 2006, 2007; Whalen & Day 2008, 2010; Riquier et al. 2010; De Vleeschouwer et al. 2012). Prior to this work, only a few studies applying MS for stratigraphic purposes of Palaeozoic sediments in the Baltoscandian region have been done. Katinas & Nawrocki (2006) presented MS correlations on Lithuanian Lower Triassic (Mesozoic)

red beds. Svensen et al. (2015) studied Upper Ordovician epicontinental subtidal marine shales and limestones including the K-bentonite in the Oslo region, Norway. They concluded that the MS log shows cycles that likely represent changes in sediment supply in response to astronomical forcing.

In a study by Plado & Kalberg (2010) MS measurements were made along the Middle and Upper Ordovician succession of the Viki core in western Estonia (Fig. 1A), 160 km SW from the Pakri Peninsula. There, the MS was measured by a handheld susceptibility meter on the surface of the core at intervals of about 7–8 cm. Although MS results, as well as the thicknesses of the formations, differ between the Viki drill core (Plado & Kalberg 2010) and the Pakri Peninsula sites (this work), the MS signal behaves in a similar manner (Fig. 2). Relatively high values are received from the Billingen and Volkhov stages and low values from the Kunda Stage and from the Lasnamägi and Uhaku stages. The positive MS excursion characteristic of the dolomitized Pae Member in the Pakri area is, however, missing in the Viki core due to differences in lithofacies within the Lasnamägi Stage. The dolomitized limestone beds are missing in the deeper-water settings further in the south and are replaced by a non-dolomitized carbonate succession.

The AMS results show a significant difference between the Pae Member dolostones and the rest of the studied limestones. The Pae Member has positive MS anomaly likely because of fluid migration-caused chemical flux, which produced secondary iron input and/or rearrangement of already existing iron and precipitation of ferroan dolomite crystals (Fig. 3B). As observed by Essalhi et al. (2009), AMS data of ferroan dolomite host rock indicates the principal direction of fluid circulation, parallel to the intermediate axis of MS ($K_{INT}$). When transferring this knowledge to the Pae Member, AMS data mean that the dolomitizing fluid flow was principally directed to SW–NE (present-day direction). Notably this direction resembles a general direction of fracture zones in the crystalline basement and in the Palaeozoic sedimentary cover in northern Estonia (Miidel 1994). Kiipli (1983) noted a link between the dolomitization of the Pae Member (and occasionally lithologies below and above) and fracture zones. The fractures are of pre-Middle Devonian age, hinting at the Late Silurian–Early Devonian as the best possible age for secondary dolomitization (Vingisaar & Taalmann 1974). It has also been suggested (Larson et al. 1999; Alm et al. 2005) that in Scandinavia the Caledonian orogenic development in the late Silurian and Devonian was responsible for the fluid event producing the fracture-controlled mineralizations. Alternatively, the Pae Member, which is distinctively followed for over 100 km along northern Estonia being likely an isochronous bed, carries dolomite due to relict (connate) marine waters (Kiipli 1983).

Dronov et al. (2011), Nielsen (2004) and Rasmussen et al. (2016) have studied sea-level history (Fig. 4) of the Baltoscandian region. According to Nielsen (2004), the succession studied here represents three 2nd-order sea-level change intervals: (i) highstand in the Billingen and early Volkhov stages, (ii) lowstand from the early Volkhov Stage to the end of the Aseri Stage and (iii) highstand starting at the base of the Lasnamägi Stage and continuing up to the Upper Ordovician. Dronov et al. (2011) divided the same interval into three 3rd-order depositional sequences: IV (Volkhov), V (Kunda) and VI (Aseri to Kukruse), hinting at relative highstands within the Volkhov and Kunda stages, but significant fluctuations and lowstands at, and near, the boundaries between the Billingen and Volkhov stages, and the Volkhov and Kunda stages, and regression at the uppermost Kunda Stage. Thus, essential differences between these two compilations exist for the Volkhov and Kunda stages, but for the Lasnamägi and Uhaku stages, the two compilations agree in transgression. A recent palaeoecological compilation by Rasmussen et al. (2016) for Dapingian and earliest Darriwilian ages shows a shift from greenhouse to icehouse, causing a major glacioeustatic sea-level drop at the Dapingian–Darriwilian (Volkhov–Kunda) transition. Considering the dependence of MS on regressive–transgressive cycles (e.g. Racki et al. 2002; Ellwood et al. 2006; Whalen & Day 2010), the present MS data do not entirely agree with the above-described compilations (Fig. 4). The only notable correlation between MS and the sea-level trend of Dronov et al. (2011) can be observed at the early–middle Volkhov time when the transgression of the sea occurred, suggesting facies shift and decrease in lithogenic input. The MS values decreasing evenly upwards (Fig. 4) could be related to the rise of sea level. At the end of the Volkhov age (Lahepere time) Dronov et al. (2011), like Rasmussen et al. (2016), hints at a regressive event. Within that interval MS, however, continues to decrease and is low during the Kunda Stage lowstand (Nielsen 2004; Rasmussen et al. 2016). Upwards along the succession, both sea-level and MS datasets are without big gradients except for high MS of the Kandle Formation and the Pae Member caused by diagenetic processes (witnessed by iron ooids and ferroan dolomite, respectively). A slight upward increase in MS during the Lasnamägi and Uhaku ages contradicts sea-level rise (Nielsen 2004; Dronov et al. 2011). We are aware that the studied sequence contains hiatuses, and correlations between MS and ≥3rd-order depositional sequences may be imperfect, but, as suggested by the results of mineralogical studies, diagenetic processes are responsible for most of the observed MS signal.

## CONCLUSIONS

Magnetic susceptibility, its frequency-dependence and the anisotropy of the Dapingian and Darriwilian sedimentary succession from three sites at the Pakri Peninsula, NW Estonia, are analysed in combination with mineralogical studies. The MS signal increases and decreases throughout the studied profile. It is, however, typical for carbonate successions worldwide, below the marine standard except for the glauconitic limestones of the Volkhov Stage and dolostones of the Pae Member. A few samples of the Kandle Formation reach higher values as well. These relatively higher susceptibilities are mostly carried by secondary Fe–Ti oxides (within the Saka Member), goethite ooids (Kandle Formation) and ferrous dolomite (Pae Member), whereas paramagnetic minerals and rare ferromagnetic detrital grains are responsible for the higher susceptibilities throughout the rest of the studied sequence. Considering the dependence of MS on regressive–transgressive cycles (generally high MS within deposits of lowstand and early transgressive episodes, and low MS within deposits of late transgressive and highstand parts of the cycles), no significant correlations with sea-level fluctuations for the Dapingian and Darriwilian ages exist, except for a correlation of MS with a sea-level compilation by Dronov et al. (2011) for the early-middle Volkhov age. Thus, in the studied case, MS cannot be used as a detrital proxy.

The measured changes in MS in the Pakri Peninsula outcrops correlate at certain characteristic levels with those deposited in the deeper part of the palaeobasin (Viki core), indicating that the post-depositional iron mobilization within the sediments took place at least at a regional level.

**Acknowledgements.** We would like to thank Olle Hints and Jaak Nõlvak from the Institute of Geology, Tallinn University of Technology for fruitful discussions. The reviewers Michael T. Whalen (Geophysical Institute, University of Alaska Fairbanks), Jindrich Hladil (Institute of Geology of the Czech Academy of Sciences) and Kalle Kirsimäe (Department of Geology, University of Tartu) are acknowledged for their helpful comments. Estonia Research Council project IUT20-34 funded JP and LA. The paper is a contribution to IGCP 591.

## REFERENCES

Ainsaar, L., Kaljo, D., Martma, T., Meidla, T., Männik, P., Nõlvak, J. & Tinn, O. 2010. Middle and Upper Ordovician carbon isotope chemostratigraphy in Baltoscandia: a correlation standard and clues to environmental history. *Palaeogeography, Palaeoclimatology, Palaeoecology*, **294**, 189–201.

Alm, E., Huhma, H. & Sundblad, K. 2005. Preliminary Palaeozoic Sm–Nd ages of fluoritecalcite-galena veins in the southeastern part of the Fennoscandian Shield. *Svensk Kärnbränslehantering AB*, R-04–27.

Alwmark, C., Schmitz, B. & Kirsimäe, K. 2010. The mid-Ordovician Osmussaar breccia in Estonia linked to the disruption of the L-chondrite parent body in the asteroid belt. *Geological Society of America Bulletin*, **122**, 1039–1046.

Bogdanova, S., Gorbatchev, R., Grad, M., Janik, T., Guterch, A., Kozlovskaya, E., Motuza, G., Skridlaite, G., Starostenko, V. & Taran, L. 2006. EUROBRIDGE: new insights into the geodynamic evolution of the East European Craton. In *European Lithosphere Dynamics* (Gee, D. G. & Stephenson, R. A., eds), *Geological Society Memoirs*, **32**, 599–625.

Crick, R. E., Ellwood, B. B., El Hassani, A., Feist, R. & Hladil, J. 1997. Magnetosusceptibility event and cyclostratigraphy (MSEC) of the Eifelian–Givetian GSSP and associated boundary sequences in north Africa and Europe. *Episodes*, **20**, 167–175.

Crick, R. E., Ellwood, B. B., El Hassani, A. & Feist, R. 2000. Proposed magnetostratigraphy susceptibility magnetostratotype for the Eifelian–Givetian GSSP (Anti-Atlas, Morocco). *Episodes*, **23**, 93–101.

Da Silva, A.-C. & Boulvain, F. 2006. Upper Devonian carbonate platform correlations and sea level variations recorded in magnetic susceptibility. *Palaeogeography, Palaeoclimatology, Palaeoecology*, **240**, 373–388.

Dearing, J. 1999. Magnetic susceptibility. In *Environmental Magnetism: A Practical Guide* (Walden, J, Oldfield, F., & Smith, J., eds), *Quaternary Research Association, London, Technical Guide*, **6**, 35–62.

De Vleeschouwer, D., Whalen, M. T., Day, J. E. & Claeys, P. 2012. Cyclostratigraphic calibration of the Frasnian (Late Devonian) time scale (western Alberta, Canada). *GSA Bulletin*, **124**, 928–942.

Dronov, A. & Holmer, E. 1999. Depositional sequences in the Ordovician of Baltoscandia. *Acta Universitatis Carolinae, Geologica*, **43**, 133–136.

Dronov, A. V., Ainsaar, L., Kaljo, D., Meidla, T., Saadre, T. & Einasto, R. 2011. Ordovician sequence of Baltoscandia: facies, sequences and sea-level changes. In *Ordovician of the World* (Gutiérrez-Marco, J. C., Rábano, I. & García-Bellido, D., eds), *Instituto Geológico y Minero de España, Madrid, Cuadernos del Museo Geominero*, **14**, 143–150.

Ellwood, B. B., Crick, R. E., El Hassani, A., Benoist, S. L. & Young, R. H. 2000. Magnetosusceptibility event and cyclostratigraphy method applied to marine rocks: detrital input versus carbonate productivity. *Geology*, **28**, 1135–1138.

Ellwood, B. B., García-Alcalde, J. L., El Hassani, A., Hladil, J., Soto, F. M., Truyóls-Massoni, M., Weddige, K. & Koptikova, L. 2006. Stratigraphy of the Middle Devonian boundary: formal definition of the susceptibility magnetostratotype in Germany with comparisons to sections in the Czech Republic, Morocco and Spain. *Tectonophysics*, **418**, 31–49.

Ellwood, B. B., Brett, C. A. & MacDonald, W. D. 2007. Magnetostratigraphy susceptibility of the Upper Ordovician Kope Formation, northern Kentucky. *Palaeogeography, Palaeoclimatology, Palaeoecology*, **243**, 42–54.

Ellwood, B. B., Tomkin, J. H., El Hassani, A., Bultynck, P., Brett, C. E., Schindler, E., Feist, R. & Bartholomew, A. J. 2011. A climate-driven model and development of a floating point time scale for the entire Middle Devonian Givetian Stage: a test using magnetostratigraphy susceptibility as a climate proxy. *Palaeogeography, Palaeoclimatology, Palaeoecology*, **304**, 85–95.

Essalhi, M., Sizaret, S., Barbanson, L., Chen, Y., Branquet, Y., Panis, D., Camps, P., Rochette, P. & Canals, A. 2009. Track of fluid paleocirculation in dolomite host rock at regional scale by the Anisotropy of Magnetic Susceptibility (AMS): an example from Aptian carbonates of La Florida, Northern Spain. *Earth and Planetary Science Letters*, **277**, 501–513.

Griffith, E. M. & Paytan, A. 2012. Barite in the ocean – Occurrence, geochemistry and paleoceanographic applicators. *Sedimentology*, **59**, 1817–1835.

Haq, B. U. & Schutter, S. R. 2008. A chronology of Palaeozoic sea-level changes. *Science*, **322**, 64–68.

Hirt, A. M., Banin, A. & Gehring, A. U. 1993. Thermal generation of ferromagnetic minerals from iron-enriched smectites. *Geophysical Journal International*, **115**, 1161–1168.

Jaanusson, V. 1973. Aspects of carbonate sedimentation in the Ordovician of Baltoscandia. *Lethaia*, **6**, 11–34.

Jelinek, V. 1981. Characterisation of the magnetic fabrics of rocks. *Tectonophysics*, **79**, 63–67.

Katinas, V. & Nawrocki, J. 2006. Application of magnetic susceptibility for correlation of the Lower Triassic red beds of the Baltic basin. *Geologija (Vilnius)*, **56**, 53–59.

Kiipli, T. 1983. Dolomites of the Estonian Middle Ordovician Väo Formation. *Proceedings of the Estonian Academy of Sciences, Geology*, **32**, 60–68.

Kirsimäe, K., Jørgensen, P. & Kalm, V. 1999. Low-temperature diagenetic illite-smectite in Lower Cambrian clays in North Estonia. *Clay Minerals*, **34**, 151–163.

Larson, S. Å., Tullborg, E.-L., Cederbom, C. & Stiberg, J.-P. 1999. Sveconorwegian and Caledonian foreland basins in the Baltic Shield revealed by fission-track thermochronology. *Terra Nova*, **11**, 210–215.

Lindström, M. 1984. The Ordovician climate based on study of carbonate rocks. *Palaeontological Contributions from the University of Oslo*, **295**, 81–88.

Lurcock, P. C. & Wilson, G. S. 2013. The palaeomagnetism of glauconitic sediments. *Global and Planetary Change*, **110**, 278–288.

Maloof, A. C., Kopp, R. E., Grotzinger, J. P., Fike, D. A., Bosak, T., Vali, H., Poussart, P. M., Weiss, B. P. & Kirschvink, J. L. 2007. Sedimentary iron cycling and the origin and preservation of magnetization in platform carbonate muds, Andros Island, Bahamas. *Earth and Planetary Science Letters*, **259**, 581–598.

Männil, R. 1966. *Evolution of the Baltic Basin During the Ordovician*. Valgus, Tallinn, 200 pp. [in Russian, with English summary].

Meidla, T., Ainsaar, L. & Tinn, O. 1998. Volkhov Stage in North Estonia and sea level changes. *Proceedings of the Estonian Academy of Sciences, Geology*, **47**, 141–157.

Miidel, A. 1994. Geological background of the present regional uplift anomaly in Estonia. *Proceedings of the Estonian Academy of Sciences, Geology*, **43**, 69–80.

Nestor, H. & Einasto, R. 1997. Formation of the territory. Ordovician and Silurian carbonate sedimentation basin. In *Geology and Mineral Resources of Estonia* (Raukas, A. & Teedumäe, A., eds), pp. 192–204. Estonian Academy Publishers, Tallinn.

Nielsen, A. T. 2004. Ordovician sea-level changes: a Baltoscandian perspective. In *The Great Ordovician Biodiversification Event* (Webby, B. D., Paris, F., Droser, M. L. & Percival, I. G., eds), pp. 84–93. Columbia University Press, New York.

Nikishin, A. M., Ziegler, P. A., Stephenson, R. A., Cloetingh, S. A. P. L., Furne, A. V., Fokin, P. A., Ershov, A. V., Bolotov, S. N., Korotaev, M. V., Alekseev, A. S., Gorbachev, V. I., Shipilov, E. V., Lankreijer, A., Bembinova, E. Yu. & Shalimov, I. V. 1996. Late Precambrian to Triassic history of the East European Craton: dynamics of sedimentary basin evolution. *Tectonophysics*, **268**, 23–63.

Orviku, K. 1940. Lithologie der Tallinna-serie (Ordovizium, Estland) I. *Acta et Commentationes Universitatis Tartuensis*, A, **36**, 1–216.

Orviku, K. 1960. Über die lithostratigraphie der Wolchow- und der Kunda-Stufe in Estland. *ENSV TA Geoloogia Instituut, Uurimused*, **5**, 45–87 [in Russian, with German summary].

Plado, J. & Kalberg, A.-L. 2010. Magnetic susceptibility of Ordovician rocks. In *Viki Drill Core* (Põldvere, A., ed.), *Estonian Geological Sections*, 10, 28–30.

Plado, J., Preeden, U., Jõeleht, A., Pesonen, L. J. & Mertanen, S. 2016. Palaeomagnetism of Middle Ordovician carbonate sequence, Vaivara Sinimäed area, northeast Estonia, Baltica. *Acta Geophysica* (accepted).

Põldsaar, K. & Ainsaar, L. 2014. Extensive soft-sediment deformation structures in the early Darriwilian (Middle Ordovician) shallow marine siliciclastic sediments formed on the Baltoscandian carbonate ramp, northwestern Estonia. *Marine Geology*, **356**, 111–127.

Põldvere, A. & Nestor, H. 2010. General geological setting and stratigraphy. In *Viki Drill Core* (Põldvere, A., ed.), *Estonian Geological Sections*, 10, 6–16.

Racki, G., Racka, M., Matyja, H. & Devleeschouwer, X. 2002. The Frasnian/Famennian boundary interval in the South Polish–Moravian shelf basins: integrated event stratigraphical approach. *Palaeogeography, Palaeoclimatology, Palaeoecology*, **181**, 251–297.

Raidla, V., Kirsimäe, K., Bityukova, L., Jõeleht, A., Shogenova, A. & Šliaupa, S. 2006. Lithology and diagenesis of the poorly consolidated Cambrian siliciclastic sediments in the northern Baltic Sedimentary Basin. *Geological Quarterly*, **50**, 395–406.

Rasmussen, C. M. Ø., Ullmann, C. V., Jakobsen, K. G., Lindskog, A., Hansen, J., Hansen, T., Eriksson, M. E., Dronov, A., Frei, R., Korte, C., Nielsen, A. T. & Harper, D. A. T. 2016. Onset of main Phanerozoic marine radiation sparked by emerging Mid Ordovician icehouse. *Scientific Reports*, **6**, 18884.

Riquier, L., Averbuch, O., Devleeschouwer, X. & Tribovillard, N. 2010. Diagenetic versus detrital origin of the magnetic susceptibility variations in some carbonate Frasnian–Famennian boundary sections from Northern Africa and Western Europe: implications for paleoenvironmental reconstructions. *International Journal of Earth Sciences*, **99**, S57–S73.

Śliwiński, M. G., Whalen, M. T., Meyer, F. J. & Majs, F. 2012. Constraining clastic input controls on magnetic

susceptibility and trace element anomalies during the Late Devonian punctata Event in the Western Canada Sedimentary Basin. *Terra Nova*, **24**, 301–309.

Sturesson, U. & Bauert, H. 1994. Origin and palaeogeographical distribution of the Viruan iron and phosphate ooids in Estonia: evidence from mineralogical and chemical compositions. *Sedimentary Geology*, **93**, 51–72.

Suk, D.-W. & Halgedahl, S. L. 1996. Hysteresis properties of magnetic spherules and whole-rock specimens from some Palaeozoic platform carbonate rocks. *Journal of Geophysical Research B: Solid Earth*, **101**, 25053–25076.

Suuroja, K., Kirsimäe, K., Ainsaar, L., Kohv, M., Mahaney, W. C. & Suuroja, S. 2003. The Osmussaar Breccia in Northwestern Estonia – evidence of a 475 Ma earthquake of an impact? In *Impact Markers in the Stratigraphic Record* (Koeberl, C. & Martinez-Ruiz, F., eds), pp. 333–347. Springer Verlag, Berlin-Heidelberg.

Svensen, H. H., Hammer, Ø. & Corfu, F. 2015. Astronomically forced cyclicity in the Upper Ordovician and U–Pb ages of interlayered tephra, Oslo Region, Norway. *Palaeogeography, Palaeoclimatology, Palaeoecology*, **418**, 150–159.

Tammekänd, M., Hints, O. & Nõlvak, J. 2010. Chitinozoan dynamics and biostratigraphy in the Väo Formation (Darriwilian) of the Uuga Cliff, Pakri Peninsula, NW Estonia. *Estonian Journal of Earth Sciences*, **59**, 25–36.

Torsvik, T. H., Van der Voo, R., Preeden, U., Mac Niocaill, C., Steinberger, B., Doubrovine, P. V., van Hinsbergen, D. J. J., Domeier, M., Gaina, G., Tohver, E., Meert, J. G., McCausland, P. J. A. & Cocks, L. R. M. 2012. Phanerozoic polar wander, palaeogeography and dynamics. *Earth-Science Reviews*, **114**, 325–368.

Vingisaar, P. & Taalmann, V. 1974. Survey of the dolomitization of the Lower Palaeozoic carbonate rocks of Estonia. *Eesti NSV Teaduste Akadeemia Toimetised, Keemia, Geoloogia*, **23**, 237–243 [in Russian, with English summary].

Whalen, M. T. & Day, J. E. 2008. Magnetic susceptibility, biostratigraphy, and sequence stratigraphy: insights into Devonian carbonate platform development and basin infilling, Western Alberta. In *Papers on Phanerozoic Reef Carbonates in Honor of Wolfgang Schlager* (Lukasik, J. & Simo, J. A., eds), *Society for Sedimentary Geology Special Publication*, **89**, 291–314.

Whalen, M. T. & Day, J. E. 2010. Cross-basin variations in magnetic susceptibility influenced by changing sea level, paleogeography, and paleoclimate: Upper Devonian, western Canada sedimentary basin. *Journal of Sedimentary Research*, **80**, 1109–1127.

## Pakri poolsaare Kesk-Ordoviitsiumi läbilõike magnetiline vastuvõtlikkus

Jüri Plado, Leho Ainsaar, Marija Dmitrijeva, Kairi Põldsaar, Siim Ots, Lauri J. Pesonen ja Ulla Preeden

On kirjeldatud Pakri poolsaare Uuga, Testepere ja Leetse paljanditest pärinevate Dapingi ja Darriwili vanusega kivimite magnetilist vastuvõtlikkust (MV), selle sõltuvust mõõtmistel kasutatava välja sagedusest ning anisotroopiat. Läbilõike MV on nõrk, kuid positiivne, viidates para- ja/või ferromagnetiliste mineraalide esinemisele. Kolmest nimetatud paljandist pärineva materjali MV muutumine vertikaalsuunas on üksteisega sarnane, andes aluse andmestiku kombineerimiseks. Andmestik sarnaneb varasemalt mõõdetud Viki puursüdamiku omaga, viidates MV sarnasusele basseini erinevates osades. Suhteliselt kõrgemad MV väärtused esinevad Toila ja Kandle kihistus ning Pae kihistikus. Mineraloogiliste vaatluste alusel on suuremad väärtused põhjustatud sekundaarsete Fe-Ti-oksiidide (Toila), götiitsete ooidide (Kandle) ja rauarikka dolomiidi (Pae) poolt. Diageneetiliste muutuste tõttu ei korreleeru MV andmestik sedimentoloogiliselt tuletatud veetaseme muutustega.